Diastereoselective Synthesis, Spectroscopy, and Electrochemistry of Ruthenium(II) Complexes of Substituted Pyrazolylpyridine Ligands

Yue Luo, Pierre G. Potvin,* Yu-Hong Tse, and A. B. P. Lever

Department of Chemistry, York University, 4700 Keele Street, North York, Ontario Canada M3J 1P3

Received June 2, 1995[⊗]

We report the synthesis of the hetero- and homoleptic ruthenium(II) complexes $Ru(bpy)_2L^{2+}$, $Ru(bpy)L_2^{2+}$ (bpy is 2,2′-bipyridine), and RuL_3^{2+} of six new bidentates L, the substituted pyrazolylpyridines **1**−**6** (1-substituted-3-(2-pyridinyl)-4,5,6,7-tetrahydroindazoles with substituents R = H, CH_3, Ph, or C_6H_4-4″-COOX where X = H, CH_3, or C_2H_5). These were fully characterized by ^{1}H- and ^{13}C-NMR spectroscopy and elemental analysis. The UV−visible spectra and redox properties of the complexes, some in the ruthenium(III) and reduced bipyridine oxidation states, are also discussed. The substituents R played a role in determining the stereochemistry of the $Ru(bpy)L_2^{2+}$ and RuL_3^{2+} products. The reaction of $Ru(DMSO)_4Cl_2$ with 3 equiv of L bearing aromatic substituents gave only meridional RuL_3^{2+} isomers. The one-step reaction of $Ru(bpy)Cl_3{\cdot}H_2O$ with 2 equiv of L provided a mixture of the three possible $Ru(bpy)L_2^{2+}$ isomers, from which one symmetric isomer (labeled β) was isolated pure. A *trans* arrangement of the pyrazole groups was deduced by ^{1}H-NMR and confirmed by X-ray crystallography for one such stereomer (β-$[Ru(bpy)(\mathbf{5})_2](PF_6)_2$, R = C_6H_4-4″-$COOC_2H_5$). In contrast, $Ru(DMSO)_4Cl_2$ reacted with 2 equiv of L and then 1 equiv of bpy to selectively form the other symmetric isomer (labeled α) where the pyridine groups of L are *trans*. Crystal data for β-$[Ru(bpy)(\mathbf{5})_2](PF_6)_2$ ($C_{52}H_{50}N_8O_4F_{12}P_2Ru$) with Mo K$\alpha$ (λ = 0.710 73 Å) radiation at 295 K: a = 28.442(13) Å, b = 18.469(15) Å, c = 23.785(9) Å, β = 116.76(0)°, monoclinic, space group $C2/c$, Z = 8. Fully anisotropic (except for H and disordered F atoms), full-matrix, weighted least-squares refinement on F^2 gave a weighted R on F^2 of 0.2573 corresponding to R on F of 0.1031 for data where $F > 4\sigma(F)$.

Introduction

The photophysical and redox properties of $Ru(bpy)_3^{2+}$ (bpy is 2,2′-bipyridine) have attracted intense interest due to its potential use as a photosensitizer, for instance in the photoinduced decomposition of water.[1] In attempts to tune the photophysical and redox properties, many analogues have been synthesized where the bipyridine ligands are replaced by other *N*,*N*′-chelating ligands. These have included substituted bipyridines,[2] benzobipyridines,[3] phenanthrolines,[4] and polyazabipyridines[5] or have featured imidazole,[6−8] thiazole,[8,9] pyrazole,[10−13] and triazole[12,14] rings. With unsymmetrical ligands L, the RuL_3^{2+} and $Ru(bpy)L_2^{2+}$ species exist as mixtures of geometric isomers.[10,11,13]

Prior to this work, several *C*-linked pyrazolylpyridine ligands were known,[15] but only two[11] have been used as ligands for Ru^{II}. We recently reported several new examples,[16] which incorporate an aliphatic ring in order to increase the lipophilicity of the complexes. In most cases, the bulkiness of the substituents was expected to favor the selective formation of the least congested isomer in octahedral complexes. Further, one of our new ligands bears an ionizable carboxy substituent which allows us to access electroneutral or anionic complexes under pH control. With some precedent in other systems,[17] we anticipated that counteracting the repulsion between positive Ru^{II} complexes and viologens in this way would permit a faster photoinduced electron transfer while reducing the need for a long excited-state lifetime. This paper presents the synthesis of homo- and heteroleptic Ru^{II} complexes of these ligands and the character-

* Corresponding author. Telephone: (416)-736-2100, ext. 66140. FAX: (416)-736-5936. E-mail: fs300111@sol.yorku.ca; BLEVER@YORKU.CA.

[⊗] Abstract published in *Advance ACS Abstracts,* August 1, 1996.

(1) Juris, A.; Balzani, V.; Barigelletti, F.; Campagna, S.; Belser, P.; von Zelewsky, A. *Coord. Chem. Rev.* **1988**, *84*, 85. Meyer, T. J. *Pure Appl. Chem.* **1986**, *58*, 1193. Kalyanasundaram, K.; Grätzel, M.; Pelizzetti, E. *Coord. Chem. Rev.* **1986**, *69*, 57.
(2) Anderson, S.; Constable, E. C.; Seddon, K. R.; Turp, J. E.; Baggot, J. E.; Pilling, M. J. *J. Chem. Soc., Dalton Trans.* **1985**, 2247. Wacholtz, W. F.; Auerbach, R. A.; Schmehl, R. S. *Inorg. Chem.* **1986**, *25*, 227. Ciana, L. D.; Hamachi, I.; Meyer, T. J. *J. Org. Chem.* **1989**, *54*, 1731.
(3) Tait, C. D.; Vess, T. M.; DeArmond, V. K.; Hanck, K. W.; Wertz, D. W. *J. Chem. Soc., Dalton Trans.* **1987**, 2467. Barigelletti, F.; Juris, A.; Balzani, V.; Belser, P; von Zelewsky, A. *Inorg. Chem.* **1987**, *26*, 4115.
(4) Anderson, S.; Seddon, K. R.; Wright, R. D.; Cocks, A. T. *Chem. Phys. Lett.* **1980**, *71*, 220. Creutz, C.; Chou, M.; Netzel, T. L.; Okumura, M.; Sutin, N. *J. Am. Chem. Soc.* **1980**, *102*, 1309. Elfring, W. H.; Crosby, G. A. *J. Am. Chem. Soc.* **1981**, *103*, 2683. Fabian, R. H.; Klassen, D. M.; Sonntag, R. W. *Inorg. Chem.* **1980**, *19*, 1977.
(5) Hunziker, M.; Ludi, A. *J. Am. Chem. Soc.* **1977**, *99*, 7370. Dose, E.; Wilson, L. J. *Inorg. Chem.* **1978**, *17*, 2660. Crutchley, R. J.; Lever, A. B. P. *J. Am. Chem. Soc.* **1980**, *102*, 7129.
(6) Atton, J. G. D. M.; Gillard, R. D. *Transition Met. Chem.* **1981**, *6*, 351.
(7) Haga, M. *Inorg. Chim. Acta* **1983**, *75*, 29.
(8) Orellana, G.; Quiroga, M. L.; Braun, A. M. *Helv. Chim. Acta* **1987**, *70*, 2073.
(9) Orellana, G.; Ibarra, C. A.; Santoro, J. *Inorg. Chem.* **1988**, *27*, 1025.
(10) Steel, P. J.; Lahousse, F.; Lerner, D; Marzin, C. *Inorg. Chem.* **1983**, *22*, 1488. House, D. A.; Steel, P. J.; Watson, A. A. *Aust. J. Chem.* **1986**, *39*, 1525.
(11) Marzin, C.; Budde, F.; Steel, P. J.; Lerner, D. *New J. Chem.* **1987**, *11*, 33.
(12) Hage, R.; Prins, R.; Haasnoot, J. G.; Reedijk, J.; Vos, J. G. *J. Chem. Soc., Dalton Trans.* **1987**, 1389.
(13) Steel, P. J.; Constable, E. C. *J. Chem. Soc., Dalton Trans.* **1990**, 1389.
(14) Hage, R.; Haasnoot, J. G.; Reedijk, J.; Vos, J. G. *Inorg. Chim. Acta* **1986**, *118*, 73. Hage, R.; Dijkhuis, A. H. J.; Haasnoot, J. G.; Prins, R.; Reedijk, J.; Buchanan, B. E.; Vos, J. G. *Inorg. Chem.* **1988**, *27*, 2185.
(15) Benckova, M.; Vegh, D.; Kovac, J.; Friedl, Z. *Chem. Pap.* **1989**, *43*, 51. *Chem. Abstr.* **111**, 194532d. Ferles, M.; Liboska, R.; Trska, P. *Collect. Czech. Chem. Commun.* **1990**, *55*, 1228. Pons, J.; Lopez, X.; Benet, E.; Casabo, J.; Teixidor, F.; Sanchez, F. J. *Polyhedron* **1990**, *9*, 2839. Brunner, H.; Scheck, T. *Chem. Ber.* **1992**, *125*, 701.
(16) Luo, Y.; Potvin, P. G. P. *J. Org. Chem.* **1994**, *59*, 1761.
(17) Gaines, G. L. *J. Phys. Chem.* **1979**, *83*, 3088.

S0020-1669(95)00694-X CCC: $12.00

Scheme 1

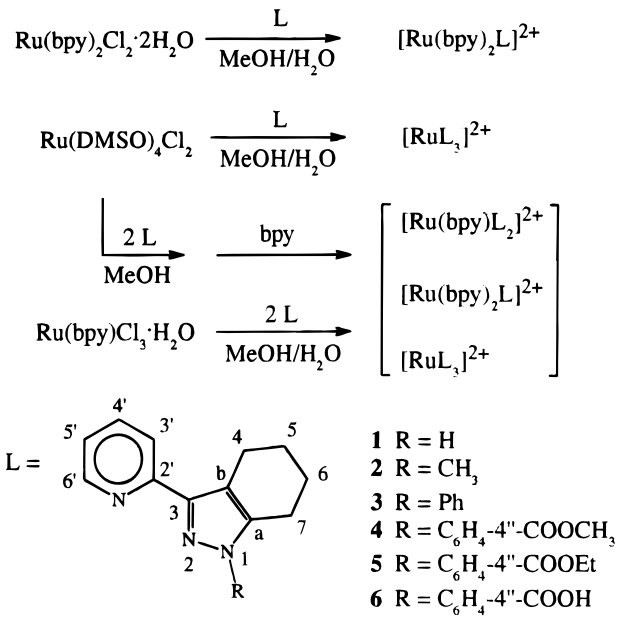

ization of the isolated geometric isomers as well as a discussion of the electronic and redox properties of the complexes in a range of oxidation states including ruthenium(III), for which spectroscopic data are comparatively rare.

Results and Discussion

Synthesis. As indicated in Scheme 1, $Ru(bpy)_2L^{2+}$ complexes were obtained as the PF_6^- salts by the reactions of *cis*-$Ru(bpy)_2Cl_2 \cdot 2H_2O$[18] with 1 equiv of ligands **1**−**6**. $Ru(DMSO)_4Cl_2$[19] was similarly treated with 3 equiv of ligand to give the homoleptic RuL_3^{2+} series, also isolated as the PF_6^- salts. Because the ligands are unsymmetrical, these homoleptic complexes can exist as *mer* and *fac* isomers. The *N*-unsubstituted **1** gave both isomers, but the *mer* isomer crystallized from MeOH−Et_2O, while the *fac* isomer remained in the mother liquor. With the other ligands **2**−**5**, the asymmetric ^{1}H- and ^{13}C-NMR spectra of the complexes indicated that only *mer* isomers had formed. We surmise that, unlike with the known *N*-linked pyridylpyrazole ligands,[13] these *C*-linked varieties bearing bulky substituents can induce significant steric crowding and destabilize the *fac* isomers.

The $Ru(bpy)L_2^{2+}$ series were prepared in two steps: an initial reaction of $Ru(DMSO)_4Cl_2$ with 2 equiv of **4**−**6**, which was complete within 4 h according to TLC, followed by a slower (1 d) reaction with 1 equiv of bpy (Scheme 1). The H_2O-insoluble PF_6^- salts of the crude products were purified by chromatography to furnish the desired $Ru(bpy)L_2^{2+}$ complexes as the major products, but this was accompanied by small amounts of the *mer*-RuL_3^{2+} and $Ru(bpy)_2L^{2+}$ species previously prepared. The ^{1}H- and ^{13}C-NMR spectra of the $Ru(bpy)L_2^{2+}$ products showed that they consisted of only one of three possible isomers, assigned by NMR (*vide infra*) and here labeled as α isomers (Figure 1). We speculate that the minor RuL_3^{2+} and $Ru(bpy)_2L^{2+}$ products arose from a small amount of ligand scrambling during the first reaction step. In an attempt to prepare $Ru(bpy)(\mathbf{5})_2^{2+}$ free of other products, a one-step reaction

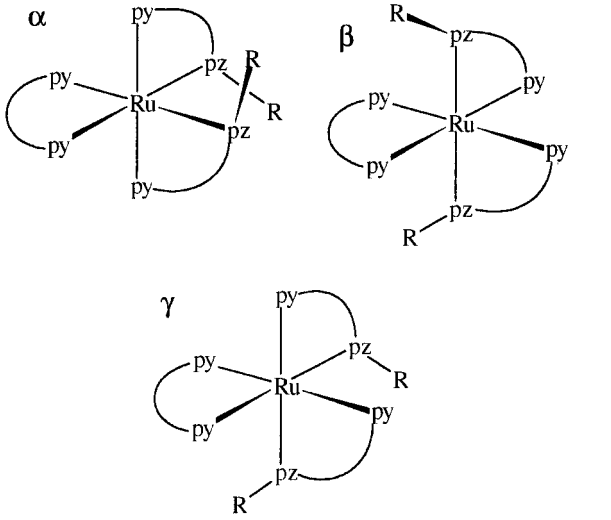

Figure 1. Geometric isomers of $Ru(bpy)L_2^{2+}$ complexes. Pyridine and pyrazole rings are represented by py and pz, respectively.

of $Ru(bpy)Cl_3 \cdot H_2O$[20] with 2 equiv of **5** was carried out, but the result was unexpected. Not only were the undesired $Ru(\mathbf{5})_3^{2+}$ and $Ru(bpy)_2(\mathbf{5})^{2+}$ contaminants again present, but $Ru(bpy)(\mathbf{5})_2^{2+}$ now consisted of all three possible isomers, labeled α, *β*, and *γ*. Their structures were assigned by NMR (*vide infra*). Some pure *β*-$[Ru(bpy)(\mathbf{5})_2](PF_6)_2$ crystallized from 1:9 MeOH−$CHCl_3$. Preparative TLC was used to isolate the remainder, and this also provided an inseparable *ca.* 1:1 mixture of the α and *γ* isomers. The diastereoselection afforded in the preparation of $[Ru(bpy)(\mathbf{5})_2](PF_6)_2$ from $Ru(DMSO)_4Cl_2$ is probably determined early, since the last incoming ligand is symmetrical bpy, whereas it is unsymmetrical **5** in the preparation from $Ru(bpy)Cl_3$.

The same geometric isomers of $[Ru(bpy)(\mathbf{6})_2](PF_6)_2$ could be similarly prepared directly from **6**, but purification by column chromatography or TLC was not possible. Instead, hydrolysis of the isolated α- and *β*-$[Ru(bpy)(\mathbf{5})_2](PF_6)_2$ furnished the corresponding pure isomers of $[Ru(bpy)(\mathbf{6})_2](PF_6)_2$.

^{1}H-NMR. Table 1 lists selected ^{1}H chemical shifts of the complexes that allowed isomer assignments. The other chemical shifts can be found in the Experimental Section. In most cases, there was much overlap of the aromatic signals and the signal assigments were only made possible by COSY spectroscopy.

Generally, the pyridine ^{1}H signals of the pyrazolylpyridine ligands lay upfield of the signals from the corresponding nuclei in bpy ligands. When the spectra of the complexes were compared with the spectra of the free ligands,[16] the effect of complexation to Ru^{II} was to shift the pyridine H-3′, H-4′, and H-5′ signals downfield (for instance by 0.02−0.22 ppm for $[Ru(bpy)_2\mathbf{2}](PF_6)_2$), as expected, while the H-6′ signal was shifted far upfield (for instance, by 1.06 ppm for $[Ru(bpy)_2\mathbf{2}](PF_6)_2$) presumably because of through-space shielding by the aromatic moieties of neighboring ligands. These observations were consistent with literature reports.[10−13] Through-space shielding also caused upfield shifts elsewhere. For example, $[Ru(\mathbf{2})_3](PF_6)_2$ showed migrations for the CH_3 peaks to positions 0.77−0.88 ppm upfield of the free ligand position. There was also an effect on the aliphatic region, as the tetrahydroindazole resonances occurred in a 2:1:1:4 integration ratio, compared to the 4:4 ratio seen with the free ligands. The upfield group is assigned to the more aliphatic *β*-CH_2 groups at positions 5 and 6 of the tetrahydroindazole moiety. Earlier work had shown

(18) Sullivan, B. P.; Salmon, D. J.; Meyer, T. J. *Inorg. Chem.* **1978**, *17*, 3334. Birchall, J. D.; O'Donoghue, T. D.; Wood, J. R. *Inorg. Chim. Acta* **1979**, *37*, L461.

(19) Evans, I. P.; Spencer, A. ; Wilkinson, G. *J. Chem. Soc., Dalton Trans.* **1973**, 204.

(20) Krause, R. A. *Inorg. Chim. Acta* **1977**, *22*, 209. Anderson, S.; Seddon, K. R. *J. Chem. Res. (S)* **1979**, 74.

Table 1. ^{1}H-NMR Chemical Shifts of Pyridine Signals

	pyrazolylpyridine				bpy			
complex	H-3′	H-4′	H-5′	H-6′	H-3	H-4	H-5	H-6
Ru(bpy)$_2$(**1**)(PF$_6$)$_2$	8.01	7.93	7.21	7.57	8.43	8.01	7.36	7.68
					8.43	8.03	7.44	7.72
					8.44	8.00	7.34	7.74
					8.47	8.01	7.41	7.77
Ru(bpy)$_2$(**2**)(PF$_6$)$_2$	8.02	7.93	7.17	7.47	8.44	8.01	7.34	7.58
					8.45	8.41	7.45	7.87
					8.46	7.98	7.33	7.79
					8.49	8.06	7.43	7.71
Ru(bpy)$_2$(**3**)(PF$_6$)$_2$	8.09	7.62	6.89	7.15	8.17	8.03	7.26	7.53
					8.36	7.96	7.32	7.52
					8.39	8.16	7.55	7.86
					8.44	8.09	7.60	8.09
Ru(bpy)$_2$(**4**)(PF$_6$)$_2$	8.03	7.56	6.78	7.09	8.16	7.99	7.20	7.51
					8.34	7.94	7.25	7.44
					8.39	8.12	7.47	7.80
					8.39	8.05	7.57	8.05
Ru(bpy)$_2$(**5**)(PF$_6$)$_2$	8.03	7.55	6.78	7.08	8.16	7.99	7.21	7.50
					8.34	7.93	7.26	7.43
					8.39	8.12	7.47	7.80
					8.39	8.05	7.57	8.05
Ru(bpy)$_2$(**6**)(PF$_6$)$_2$	8.04	7.59	6.80	7.10	8.17	7.99	7.21	7.51
					8.34	7.94	7.25	7.44
					8.40	8.11	7.47	7.81
					8.40	8.05	7.57	8.05
α-Ru(bpy)(**4**)$_2$(PF$_6$)$_2$	7.48	7.48	6.80	7.03	8.31	7.99	7.41	7.96
α-Ru(bpy)(**5**)$_2$(PF$_6$)$_2$	7.48	7.48	6.81	7.03	8.30	7.98	7.41	7.94
β-Ru(bpy)(**5**)$_2$(PF$_6$)$_2$	7.70	7.61	7.00	7.39	8.11	8.02	7.40	7.97
γ-Ru(bpy)(**5**)$_2$(PF$_6$)$_2$	8.00	7.88	7.10	7.21	8.14	8.03	7.37	7.64
	7.78	7.55	7.11	7.66	8.13	8.09	7.30	7.68
α-Ru(bpy)(**6**)$_2$(PF$_6$)$_2$	7.51	7.51	6.81	7.04	8.31	8.00	7.42	7.96
β-Ru(bpy)(**6**)$_2$(PF$_6$)$_2$	7.74	7.65	7.02	7.40	8.10	8.01	7.40	7.98
mer-Ru(**1**)$_3$(PF$_6$)$_2$	7.95	7.88	7.21	7.60				
	7.95	7.89	7.23	7.51				
	7.97	7.90	7.17	7.64				
fac-Ru(**1**)$_3$(PF$_6$)$_2$	7.95	7.88	7.16	7.51				
mer-Ru(**2**)$_3$(PF$_6$)$_2$	7.96	7.91	7.22	7.51				
	7.97	7.88	7.22	7.73				
	8.01	7.90	7.20	7.59				
mer-Ru(**3**)$_3$(PF$_6$)$_2$	7.35	7.61	6.93	7.27				
	7.67	7.55	7.06	7.37				
	7.97	7.90	7.26	7.78				
mer-Ru(**4**)$_3$(PF$_6$)$_2$	7.32	7.61	6.99	7.31				
	7.68	7.54	7.11	7.33				
	8.00	7.93	7.27	7.82				
mer-Ru(**5**)$_3$(PF$_6$)$_2$	7.32	7.60	6.99	7.31				
	7.69	7.54	7.12	7.33				
	7.99	7.92	7.27	7.80				
mer-Ru(**6**)$_3$(PF$_6$)$_2$[a]	7.31	7.68	7.16	7.31				
	7.75	7.61	7.24	7.36				
	8.09	8.02	7.40	7.40				

[a] In DMSO-d_6.

that complexation to Na^+, Zn^{2+}, or H^+ causes a differentiation between the α-CH_2 groups at positions 4 and 7.[16,21] In the Ru^{II} complexes, the more downfield resonance (near 3.0 ppm) was readily assigned by NOE difference spectroscopy to the nonequivalent CH_2-4 nuclei, as only irradiation there produced an enhancement of the neighboring pyridine H-3′ signal. Through-space shielding appeared to therefore cause a further differentiation of the individual ^{1}H signals from those at position 7, which lay more upfield.

Phenyl resonances were also affected by complexation. There was a strong differentiation of the diastereotopic 2″ and 6″ (or *ortho*) nuclei and, to a lesser degree, of the *meta* (3″ and 5″) nuclei. For instance, [Ru(bpy)$_2$**5**](PF$_6$)$_2$ exhibited one *ortho* signal lying 1.88 ppm upfield of the free ligand position, while the other had migrated by 0.71 ppm. Similarly, the homoleptic but asymmetric complex *mer*-[Ru(**5**)$_3$](PF$_6$)$_2$ gave rise to very complicated spectra, but three relatively high field signals (at 6.05, 6.43, and 6.55 ppm) were readily discerned and assigned to the most shielded ^{1}H of each *ortho* pair. Thus, one edge of each phenyl ring, twisted out of the pyrazolylpyridine plane, appears to lie closer to the shielding source.

^{13}C-NMR. Because of their greater spread, the ^{13}C-NMR assignments were straightforward except for overlaps between some bpy signals that were resolved by two-dimensional ^{13}C−^{1}H shift-correlation spectroscopy in some cases. The chemical shifts of the aromatic signals and their assignments appear in the Supporting Information. In all cases, the chemical shifts were downfield of the free ligand positions. In contrast to ^{1}H-NMR spectra, there was little evidence of through-space shielding effects in operation.

Structures of the Ru(bpy)L$_2^{2+}$ Isomers. As related earlier, two isomers (α and β) of [Ru(bpy)(**5**)$_2$](PF$_6$)$_2$ were obtained pure while the third (γ) was obtained in a mixture with the α form. The ^{1}H-NMR spectra of the α and β isomers were symmetrical but quite different. That of the γ form, obtained by spectroscopic subtraction, was asymmetric, and the γ form was therefore assigned the only possible asymmetric structure (Figure 1). The structures of the α and β isomers were deduced from three differences in their ^{1}H spectra: (i) the pyridine signals from ligand **5** in the α isomer lay somewhat upfield of the corresponding signals in the β isomer; (ii) one *ortho* signal and one *meta* signal from the β form were shifted further upfield by through-space shielding than with the α isomer, while the other *ortho* and the other *meta* signals were at comparable positions; and (iii) the bpy H-3 signal from the β isomer was further upfield than the corresponding signal from the α form, while the other bpy signals were at comparable positions. According to our general observations (*vide supra*), these differences implied that the β isomer enabled a stronger ligation of **5** through weaker interligand steric interactions and stronger mutual, through-space shielding interactions between **5** and bpy. Both are available with the structure drawn for the β form in Figure 1.

This assignment was confirmed by X-ray crystallography of β-[Ru(bpy)(**5**)$_2$](PF$_6$)$_2$ (Figure 2). This showed a distorted octahedron, presumably because of the interaction between the bipyridine and phenyl rings. Indeed, the phenyl rings are twisted out of the pyrazolylpyridine planes with angles of 76.8 and 88.2°, respectively, placing them nearly parallel above and below the bpy plane. In confirmation of our NMR spectral analysis, such π-stacking would be expected to give the observed mutual shielding interactions. By implication and by spectral similarities to α-[Ru(bpy)(**5**)$_2$](PF$_6$)$_2$, the structures of α-[Ru(bpy)(**4**)$_2$](PF$_6$)$_2$ and α-[Ru(bpy)(**6**)$_2$](PF$_6$)$_2$ were ascertained.

Electrochemistry. (See Table 2 and, Figure S-1 (Supporting Information).) The cyclic voltammetric (CV) behavior of the RuL$_3^{2+}$ complexes was very similar to that of Ru(bpy)$_3^{2+}$. At low temperature, RuL$_3^{2+}$ species in THF showed three reversible, one-electron reduction processes corresponding with successive reductions of each L. However, at room temperature (in most cases), only the first reduction was reversible, while no reversible reduction process was observed for the *N*−H complex [Ru(**1**)$_3$](PF$_6$)$_2$. The RuL$_3^{2+}$ complexes were about 0.5 V more difficult to reduce than Ru(bpy)$_3^{2+}$, suggesting relatively higher-lying ligand π* orbitals. The spacings between the reduction steps were larger (230 and 350 mV) than the corresponding spacings with Ru(bpy)$_3^{2+}$ (180 and 230 mV), suggesting stronger interligand repulsions. RuL$_3^{2+}$ in CH_3CN showed one reversible oxidation wave assigned to the $Ru^{3+/2+}$ couple[22] and observed about 100−200 mV more negative than with Ru(bpy)$_3^{2+}$. The lower oxidation potential with [Ru(**1**)$_3$]-

(21) Van der Valk, P.; Potvin, P. G. P. *J. Org. Chem.* **1994**, *59*, 1766.

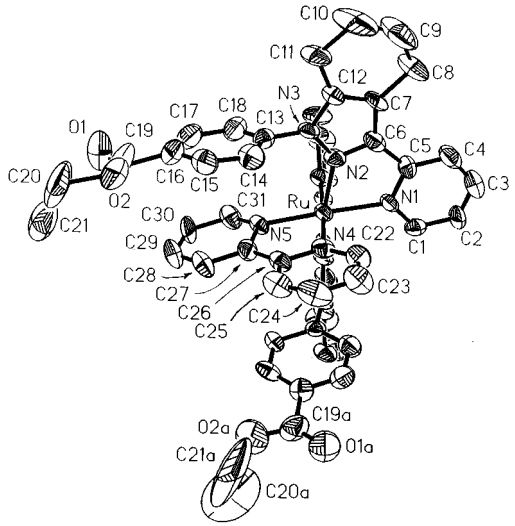

Figure 2. ORTEP plot of the X-ray crystal structure of β-Ru(bpy)-(**5**)$_2$(PF$_6$)$_2$. For clarity, H and PF$_6$ atoms are not shown, and 25% probability thermal ellipsoids are presented. The numbering sequence for both units of **5** is the same. Selected bond lengths (Å): Ru−N1, 2.078(13); Ru−N2, 2.077(12); Ru−N1a, 2.072(14); Ru−N2a, 2.039-(12); Ru−N4, 2.031(14); Ru−N5, 2.061(13). Seleted bond angles (in deg): N1−Ru−N2, 77.3(6); N1a−Ru−N2a, 76.8(6); N4−Ru−N5, 78.4(6); N2−Ru−N2a, 166.7(6); N1−Ru−N5, 177.3(5); N1a−Ru−N4, 176.3(6); N1−Ru−N1a, 84.2(5); N1−Ru−N2a, 92.0(5); N1−Ru−N4, 99.2(6); N2−Ru−N1a, 94.1(5); N2−Ru−N4, 85.5(5); N2−Ru−N5, 103.8(6); N1a−Ru−N5, 98.2(6); N2a−Ru−N4, 104.2(5); N2a−Ru−N5, 87.3(5).

Table 2. Half-Wave Potentials[a]

complex	$E^{3+/2+}$	$E^{2+/1+}$	$E^{1+/0}$	$E^{0/1-}$
mer-Ru(**1**)$_3$(PF$_6$)$_2$	0.93			
mer-Ru(**2**)$_3$(PF$_6$)$_2$	1.03	−1.78	−2.02	
mer-Ru(**2**)$_3$(PF$_6$)$_2$[b]		−1.80	−2.03	−2.38
mer-Ru(**3**)$_3$(PF$_6$)$_2$	1.03	−1.73		
mer-Ru(**3**)$_3$(PF$_6$)$_2$[c]		−1.74	−2.04	−2.34
mer-Ru(**4**)$_3$(PF$_6$)$_2$	1.12	−1.67		
mer-Ru(**5**)$_3$(PF$_6$)$_2$	1.12	−1.66		
α-Ru(bpy)(**5**)$_2$(PF$_6$)$_2$	1.11	−1.34		
β-Ru(bpy)(**5**)$_2$(PF$_6$)$_2$	1.18	−1.45		
Ru(bpy)$_2$**1**(PF$_6$)$_2$	1.15	−1.49	−1.74	
Ru(bpy)$_2$**2**(PF$_6$)$_2$	1.19	−1.32		
Ru(bpy)$_2$**3**(PF$_6$)$_2$	1.20	−1.34	−1.61	
Ru(bpy)$_2$**4**(PF$_6$)$_2$	1.23	−1.34	−1.58	−2.06
Ru(bpy)$_2$**5**(PF$_6$)$_2$	1.23	−1.33	−1.57	−2.04
Ru(bpy)$_2$**6**(PF$_6$)$_2$	1.23	−1.35	−1.65	−2.18
Ru(bpy)$_3^{2+}$[d]	1.24	−1.34	−1.52	−1.75

[a] Potentials are given in V vs SCE, and all waves are reversible; CH_3CN containing 0.1 M (TBA)PF$_6$ as the supporting electolyte; T = 20 ± 1 °C. [b] In THF at −23 ± 1 °C. [c] In THF at −85 ± 1 °C. [d] At 23 ± 1 °C. From: Amira-Soriaga, L.; Sprouse, S. D.; Watts, R. J.; Kaska, W. C. *Inorg. Chim. Acta* **1984**, *84*, 135.

(PF$_6$)$_2$ could be ascribed to a deprotonated species, as this is not unusual for complexes bearing ionizable N−H.[7,12]

The CV plots of most Ru(bpy)$_2$L^{2+} species showed two reversible reduction couples at room temperature. The less well defined third reduction process was also observed. Only one reversible reduction was observed with [Ru(bpy)$_2$**2**](PF$_6$)$_2$. From a comparison with RuL$_3^{2+}$ species and with Ru(bpy)$_3^{2+}$, the first two reductions of Ru(bpy)$_2$L^{2+} could be attributed to reduction processes at the bpy ligands. The third wave probably involves reduction of L since further reduction of bpy$^{\bullet-}$ ligands would be expected to occur at much more negative potentials (about 1 V more negative than the first wave).[23] Extended Hückel calculations, with charge iteration[24−26] were consistent with this supposition. All Ru(bpy)$_2$L^{2+} species showed one reversible, well-defined Ru$^{III/II}$ couple at about 1.2 V. Sample CV plots are given in the Supporting Information.

Ligand electrochemical parameters,[27] E_L(L), were extracted from the data in Table 2. All the data are consistent with E_L-(L) = 0.21 V for **1**−**3** and E_L(L) = 0.22 V for **4**−**6**. These data, not surprisingly, are more consistent with these ligands behaving like substituted pyridines rather than like bipyridine analogues; *i.e.*, they are somewhat poorer acceptors than bipyridine.

Electronic Spectra. (See Table 3, Figures 3−6, and Figure S-2 (Supporting Information)). The assignment of the electronic spectra was approached by consideration of the previous literature on the spectra of species of this type but also by oscillator strength calculations[28] based upon the Extended Hückel calculations,[24−26] referred to here conveniently as EHT-f calculations.

Considering the initial Ru(II) species (Figure 3), the higher-energy bands (240−290 nm) were assigned to $\pi \rightarrow \pi^*$ transitions since the free ligands also showed transitions in that region. The bands around 410 nm can be assigned to the $d\pi \rightarrow \pi^*$(L) transition and the bands at 450 nm to the $d\pi \rightarrow \pi^*$(bpy) transition by comparison with those of the *N*-linked pyrazolylpyridine Ru^{II} analogues[10−13] and Ru(bpy)$_3^{2+}$ and by consistency with the EHT-f calculations. The mixed-ligand complexes gave rise to two such bands. For Ru(bpy)L$_2^{2+}$, the relatively higher intensity of the bands at 410 nm is attributed to the higher population of the corresponding $d\pi \rightarrow \pi^*$(L) components. According to the electrochemical data, the π^* levels of L are at higher energies and the lower energy band could therefore be assigned to a $d\pi \rightarrow \pi^*$(bpy) transition. In general, the 30−40 nm difference between this and the $d\pi \rightarrow \pi^*$(L) transition is entirely in line with the 300−400 mV difference predicted by the electrochemical data. Aromatic substituents apparently had negligible effects on the positions of the MLCT and $\pi \rightarrow \pi^*$ transitions, indicating no significant overlap between the phenyl group and the π system of the pyrazolylpyridine moiety, as had been suggested by NMR.

Spectroelectrochemistry. No detailed study of the electronic spectra of these species in their oxidized or reduced forms was carried out, but several representative examples were studied. Their UV−visible absorption bands and molecular extinction coefficients are listed in Table 3 for [Ru(bpy)$_2$**5**](PF$_6$)$_2$ and [Ru-(**2**)$_3$](PF$_6$)$_2$. The disappearance of the MLCT band at 400−460 nm, the appearance of LMCT bands in the region 480−700 nm, and the shifting of the $\pi \rightarrow \pi^*$ bands to the red are characteristic of the formation of a Ru^{III} species.[29] Ruthenium-

(22) Tokel-Takvoryan, N. E.; Hemingway, R. E.; Bard, A. J. *J. Am. Chem. Soc.*, **1973**, *95*, 6582.
(23) Ohsawa, Y.; Hanck, K. W.; DeArmond, M. K. *J. Electroanal. Chem. Interfacial Electrochem.* **1984**, *175*, 229.
(24) Hoffmann, R.. *J. Chem. Phys.* **1963**, *37*, 1397. Hoffmann, R.; Lipscomb, W. N. *J. Chem. Phys.* **1962**, *36*, 2179, 3489; **1962**, *37*, 2872.
(25) Viste, A.; Gray, H. B. *Inorg. Chem.* **1964**, *3*, 1113.
(26) *Spartan v.3.1.2*, Wavefunction Inc.: 18401 Von Karman, Suite 370, Irvine CA 92715.
(27) (a) Lever, A. B. P. *Inorg. Chem.* **1990**, *29*, 1271. Lever, A. B. P. *Inorg. Chem.* **1991**, *30*, 1980. (b) Lever, A. B. P. In *Proceedings of the NATO Advanced Workshop—Molecular Electrochemistry of Inorganic, Bioinorganic and Organometallic Compounds*, Sintra Portugal; Pombeiro, A. J. L., McCleverty, J. A., Eds.; Kluwer Publishing: March 1992; p 41. (c) Masui, H.; Lever, A. B. P. *Inorg. Chem.* **1993**, *32*, 2199.
(28) Fielder, S. S.; Lever, A. B. P. ; Pietro, W. J. Paper in preparation.
(29) (a) Bryant, G. M.; Fergusson, J. E. *Aust. J. Chem.* **1971**, *24*, 275.1. Benedix, R.; Hennig, H. *Z. Chem.* **1990**, *30*, 220. (b) Crutchley, R. J.; Mccaw, K.; Lee, F. L.; Gabe, E. J. *Inorg. Chem.* **1990**, *29*, 2576. (c) Ludi, A. *Inorg. Chem.* **1975**, *14*, 1902.

Table 3. UV−Visible Absorption Maxima[a,b]

complex	$\pi \rightarrow \pi^*$		MLCT		
mer-Ru(**1**)$_3$(PF$_6$)$_2$	240 (4.59)	286 (4.64)		412 (4.20)	
mer-Ru(**2**)$_3$(PF$_6$)$_2$	245 (4.56)	290 (4.67)		408 (4.17)	
mer-Ru(**3**)$_3$(PF$_6$)$_2$	246 (4.57)	291 (4.70)		409 (4.16)	
mer-Ru(**4**)$_3$(PF$_6$)$_2$	247 (4.63)	292 (4.66)		410 (4.08)	
mer-Ru(**5**)$_3$(PF$_6$)$_2$	247 (4.72)	291 (4.76)		411 (4.19)	
α-Ru(bpy)(**5**)$_2$(PF$_6$)$_2$	248 (4.61)	288 (4.77)		398 (4.01)	450 (3.87)
β-Ru(bpy)(**5**)$_2$(PF$_6$)$_2$	242 (4.63)	290 (4.75)	372 (3.86)	408 (4.03)	450 (3.83)
Ru(bpy)$_2$**1**(PF$_6$)$_2$	242 (4.45)	288 (4.77)	382 (3.85)	416 (3.94)	454 (3.97)
Ru(bpy)$_2$**2**(PF$_6$)$_2$	243 (4.48)	287 (4.87)	381 (3.82)	412 (4.00)	449 (4.05)
Ru(bpy)$_2$**3**(PF$_6$)$_2$	243 (4.50)	287 (4.84)	383 (3.79)	418 (3.99)	449 (4.00)
Ru(bpy)$_2$**4**(PF$_6$)$_2$	242 (4.51)	287 (4.81)	381 (3.76)	414 (3.97)	453 (3.97)
Ru(bpy)$_2$**5**(PF$_6$)$_2$	243 (4.61)	286 (4.89)	380 (3.75)	420 (4.14)	450 (4.15)
Ru(bpy)$_2$**6**(PF$_6$)$_2$	242 (4.54)	287 (4.83)	384 (3.82)	418 (4.00)	449 (4.00)
Ru(bpy)$_3^{2+}$ [c]	238 (4.48)	250 (4.40)	323 (3.81)	345 (3.81)	451 (4.15)
	285 (4.94)				
Ru(**2**)$_3^{3+}$	251 (4.50)	305 (4.58)	467 (3.62)[d]	614 (3.65)[d,e]	
Ru(bpy)$_2$**5**$^{3+}$	248 (4.66)	306 (4.67)	316 (4.65)[d,f]	574 (3.67)[d]	
Ru(bpy)$_2$**5**$^{1+}$	244 (4.62)	294 (4.77)	362 (4.40)[g]	488 (4.16)[h]	
Ru(bpy)$_2$**5**^{0}	248 (4.58)	296 (4.67)	358 (4.57)[g]	502 (4.29)[h]	

[a] CH_3CN as solvent. [b] Wavelength in nm and log ϵ indicated in parentheses. [c] From: Crutchley, R. J.; Lever, A. B. P. *Inorg. Chem.* **1982**, *21*, 2276. [d] LMCT transition. [e] Broad. [f] Shoulder. [g] Assignment unknown; probably $\pi \rightarrow \pi^*$ bpy$^-$. [h] Composite band; MLCT etc.—see text for assignment.

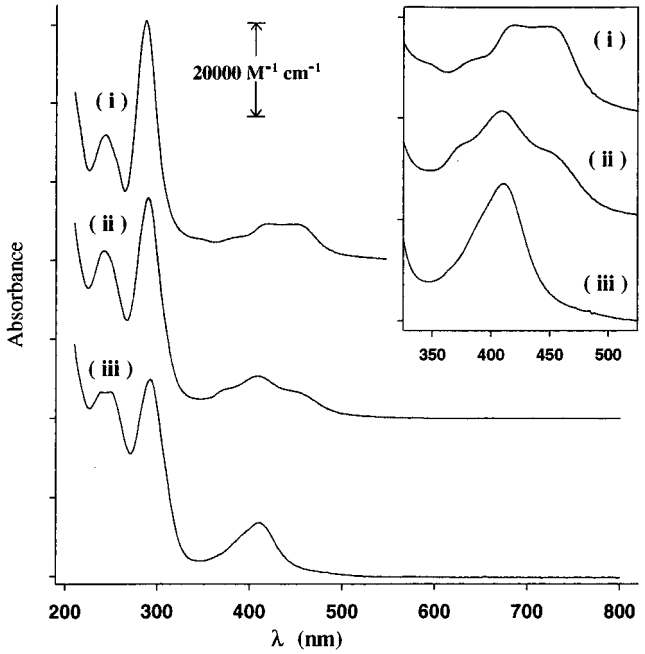

Figure 3. UV−visible spectra of (i) Ru(bpy)$_2$**5**(PF$_6$)$_2$, (ii) *β*-Ru(bpy)(**5**)$_2$(PF$_6$)$_2$, and (iii) Ru(**5**)$_3$(PF$_6$)$_2$ in acetonitrile.

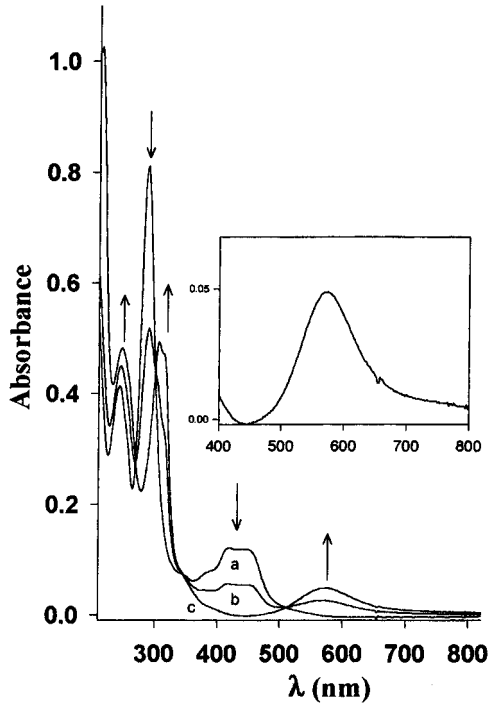

Figure 4. Spectroscopic changes during the oxidation of Ru(bpy)$_2$**5**(PF$_6$)$_2$ in CH_3CN containing 0.2 M (TBA)PF$_6$: (a) initial spectrum without applying potential; (b) first scan after polarizing the potential at 1.5 V vs AgCl/Ag for 1 min; and (c) final spectrum at 1.5 V. Inset: Expanded low-energy spectrum of spectrum c. The little dip near 650 nm in Figures 4−6 is an instrumental artifact.

(III) diimine species are usually unstable so that the observation of their electronic spectra is not well documented in the literature.

In the spectrum (Figure 5) of Ru(**2**)$_3^{3+}$ there appear to be bands near 610 and 467 nm which are identified with $\pi \rightarrow d\pi^*$ transitions to the "hole" in the Ru^{III} t_{2g} (in octahedral stereochemistry) presumably from different ligand π levels. Indeed, EHT-f calculations predict six such π(L) $\rightarrow$ d transitions clustered together with a total oscillator strength of about 0.06; these presumably lie underneath the experimental band envelope which evidently contains at least three transitions (see inset to Figure 5; experimental oscillator strengths are approximately 0.08 and 0.04 for the lower and higher energy bands, respectively).

The spectrum (Figure 4) of the Ru^{III} complex Ru(bpy)$_2$**5**$^{3+}$ has similar features, a shift to the red of the $\pi \rightarrow \pi^*$ band, a loss of the MLCT transition, and a new low-energy absorption associated with LMCT transitions. Reference to the inset to Figure 4 suggests there are probably at least two LMCT transitions. EHT-f calculations predict a low lying π(L) $\rightarrow$ d transition followed by a cluster of mixed π(L) and π(bpy) $\rightarrow$ d transitions, four in all, of overall calculated oscillator strength ca. 0.04. The experimental value is ca. 0.07.

Mixing between the Ru dπ levels and the ligand π levels is significant, with EHT calculations revealing that the half-empty dπ orbital is only 66% centered on Ru in the Ru(L)$_3^{3+}$ species and 71% in the Ru(bpy)$_2$L^{3+} species. The ability of some ligands to form strong π bonds with the t_{2g} set of Ru^{III} was recently explored,[30,31] and the aspect of Ru d orbital involvement with diimine ligand π and π^* orbitals is under active analysis.[32]

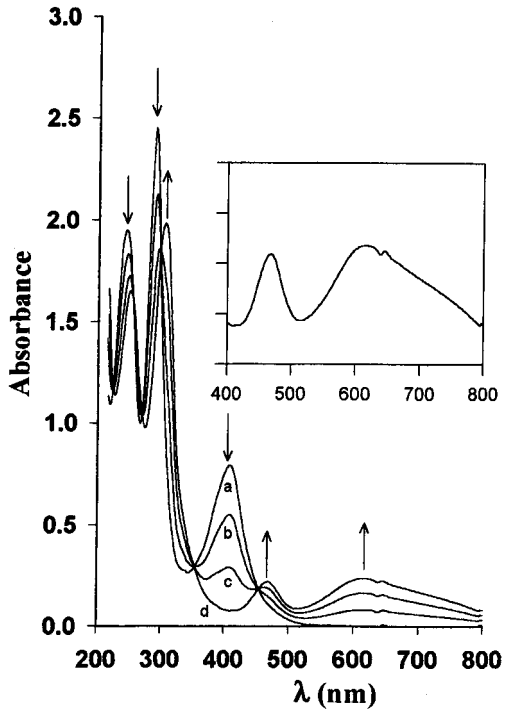

Figure 5. The spectroscopic changes during the oxidation of complex $Ru(\mathbf{2})_3(PF_6)_2$ in CH_3CN containing 0.2 M $(TBA)PF_6$: (a) initial spectrum without applying potential; (b) first scan after polarizing the potential at 1.6 V vs AgCl/Ag; (c) spectrum taken 3 min after (b); (d) final spectrum at 1.6 V. Inset: Expansion of the low-energy range of the fully oxidized species.

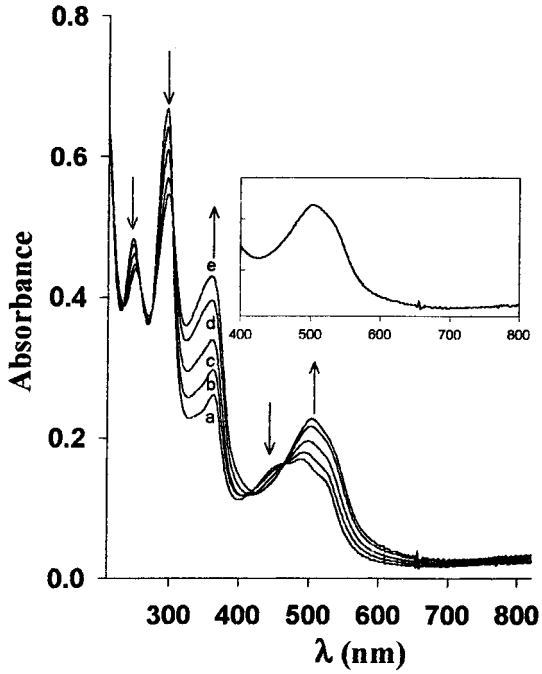

Figure 6. Spectroscopic changes during the reduction of $[Ru(bpy)_2\mathbf{5}]^+$ in CH_3CN containing 0.2 M $(TBA)PF_6$: (a) at −1.8 V; (b) at −1.85 V; (c) at −1.9 V; (d) at −1.95 V; (e) at −2.0 V vs AgCl/Ag. Note that the initial spectrum (a) corresponds to that of the monocation $[Ru(bpy)_2\mathbf{5}]^+$ and the final spectrum (e) to that of $[Ru(bpy)_2\mathbf{5}]$. Inset: Expanded low-energy region of spectrum (e).

Attempts to obtain the spectrum of the reduced form of $Ru(\mathbf{2})_3^{2+}$ were not successful due to decomposition of the complex. However, the first and second reduced forms of $Ru(bpy)_2\mathbf{5}^{2+}$ are stable. Both species can be electrochemically oxidized back quantitatively to $Ru(bpy)_2\mathbf{5}^{2+}$ during the time scale of the spectroelectrochemical measurement. The spectra of reduced Ru and other metal diimine complexes have been reported extensively[33−35] and are usually interpreted in terms of a localized picture where, with the first reduced species, for example, the complex has two unreduced ligands and one reduced ligand bound to Ru^{II}. As reduction proceeds, the $\pi \rightarrow \pi^*$ band of the diimine ligand diminishes and a new $\pi \rightarrow \pi^*$ band associated with the reduced ligand arises just to the red of the former band (Figure S2 (Supporting Information) and Figure 6, spectrum a). The MLCT band generally splits into at least two bands to the red of the initial MLCT band in the Ru^{II} species; one of these two bands, usually the higher energy one, is assigned to the $d\pi \rightarrow \pi^*$(diimine) transition of the diimine which is not reduced, while the lower energy component-(s) is (are) assigned to a low-lying $d\pi \rightarrow \pi^*$ transition of the reduced ligand; the latter band increases in intensity as the complex is sequentially reduced, while the former band diminishes in intensity.[34,35] The red shift of the MLCT band is associated with the increase in electron density on the ruthenium center due to binding to the reduced ligand.

These characteristics are well reproduced in the spectra of the first and second reduced forms of $Ru(bpy)_2\mathbf{5}^{2+}$ (Figure 6, Figure S-2 (Supporting Information)) and are consistent in this case with reduction at the bipyridine rather than at the pyrazolylpyridine ligand as anticipated from the relative reduction potentials. EHT calculation confirm reduction at the bipyridine ligand. No oscillator strength calculations were carried out on the singly reduced species, since there is no geometry optimization in the EHT model to localize the odd electron on one bpy ligand as experimentally anticipated. For the doubly reduced species, however, EHT places an electron on each bpy and predicts a cluster of $d\pi \rightarrow \pi^*$(L) and $d\pi \rightarrow \pi^*$(bpy) transitions with the lowest intense MLCT band being mainly localized as $d\pi \rightarrow \pi^*$ (bpy^-) as anticipated. The inset in Figure 6 confirms the composite nature of this lowest energy MLCT transition. The experimental total oscillator strength of this band is about 0.47 compared with a predicted theoretical value of 0.26. Given the crudity of the wave functions generated by the EHT model, this order of magnitude agreement is acceptable.

Summary and Conclusion

The substituted pyrazolylpyridines described herein formed complexes of the type $Ru(bpy)_2L^{2+}$, $Ru(bpy)L_2^{2+}$, and RuL_3^{2+} with no particular difficulty. With large substituents, only single isomers of the last two types formed (α and *mer*, respectively). Compared to those of $Ru(bpy)_3^{2+}$, the new ligands rendered the complexes a little easier to oxidize and somewhat more difficult to reduce, while their MLCT bands were blue-shifted by 30−40 nm with little influence from aromatic substituents.

Spectroelectrochemical methods revealed the spectra of two ruthenium(III)-containing oxidation products and a singly and doubly reduced species. The LMCT bands in the former and MLCT bands in the latter and in the parent species are composite

(30) Zhang, L. T.; Ondrechen, M. J. *Inorg. Chim. Acta* **1995**, *226*, 43.
(31) LaChance-Galang, K. J.; Doan, P. E.; Clarke, M. J.; Rao, U.; Yamano, A.; Hoffman, B. M. *J. Am. Chem. Soc.* **1995**, *117*, 3529.
(32) Vlček , A. A.; Pietro, W. J.; Fielder, S. S.; Lever, A. B. P. Paper in preparation.
(33) Berger, R. M.; McMillin, D. R. *Inorg. Chem.* **1988**, *27*, 4245. Krejčík, M.; Vlček, A. A. *Inorg. Chem.* **1992**, *31*, 2390. Elliott, C. M.; Hershenhart, E. *J. Am. Chem. Soc.* **1982**, *104*, 7519. Záliš, S.; Krejčík,, M.; Drchal, V.; Vlček, A. A. *Inorg. Chem.* **1995**, *34*, 6008.
(34) Donohoe, R. J.; Tait, C. D.; DeArmond, M. K.; Wertz, D. W. *Spectrochim. Acta, Part A* **1986**, *42A*, 233. Donohoe, R. J.; Tait, C. D.; DeArmond, M. K.; Wertz, D. W. *J. Phys. Chem.* **1986**, *90*, 3923.
(35) Braterman, P. S.; Song, J. I.; Peacock, R. D. *Inorg. Chem.* **1992**, *31*, 555. Braterman, P. S.; Song, J. I.; Peacock, R. D. *Spectrochim. Acta* **1992**, *48*, 899.

in nature and can be understood in terms of the electronic structures of the complexes and utilizing extended Hückel theory expanded to predict oscillator strengths.

According to the crystal structure of β-[Ru(bpy)(**5**)$_2$](PF$_6$), the complex β-[Ru(bpy)(**6**)$_2$](PF$_6$) will be well suited, in ionized form, to a close supramolecular association with viologens because the distance between the two carboxyl carbons (9.54 Å in β-[Ru(bpy)(**5**)$_2$](PF$_6$)) can comfortably accommodate a viologen, in which the distance between the two pyridinium nitrogens atoms is about 7.8 Å. The electrochemical and spectral results suggest that the bipyridine ring of β-[Ru(bpy)-(**6**)$_2$](PF$_6$) should be best able to relay an electron from Ru^{II} to a viologen. According to the structure of β-[Ru(bpy)(**5**)$_2$](PF$_6$)$_2$, the bpy will be in close proximity to the supramolecularly bound viologen, as it lies between the two parallel carboxyphenyl groups at a 34° angle from the carboxy-to-carboxy axis. Work is currently underway to demonstrate and exploit this supramolecular association.

Experimental Section

General Procedures. The precursors *cis*-Ru(bpy)$_2$Cl$_2$·2H$_2$O,[18] Ru(DMSO)$_4$Cl$_2$[19] and Ru(bpy)Cl$_3$·H$_2$O[20] were prepared according to literature procedures. The new ligands were prepared as previously reported.[16] *n*-Bu$_4$NPF$_6$ (Aldrich) was recrystallized from absolute EtOH and dried in a vacuum oven at 120 °C for 1 d. CH$_3$CN was fractionally distilled from P$_2$O$_5$. THF was distilled over Na and benzophenone. Column chromatography used neutral Al$_2$O$_3$, while TLC was carried out on E. Merck DC-Plastikfolien aluminium oxide 60 F$_{254}$ plates.

^{1}H- and ^{13}C-NMR spectra were recorded on a Bruker AMX-400 spectrometer in CD$_3$CN. In this section and in Tables 1 and S-6 (Supporting Information), the assignments use the indazole numbering (see Scheme 1) with primed positions referring to the 3-linked pyridine group and doubly primed positions referring to phenyl substituents. The values reported in this section are those not appearing in the tables. Cyclic voltammetry (CV) was performed using a Pine Instruments RDE-3 potentiostat. A conventional three-electrode cell was used in all experiments. The working electrode was a Pt disk (0.196 mm^2), and the quasi-reference electrode was Ag or Ag/AgCl wire. A Pt wire was used as a counter electrode. Ferrocene was added at the end of each experiment to serve as the internal reference. Its potential was taken to be +0.425 V vs SCE. UV−visible spectra were recorded with Varian-2400 or HP-Model 8452A diode array spectrophotometers. The spectroelectrochemical cell was based on the design of Krejcik et al.[36] and was modified as described in ref.[37] Extended Hückel calculations[24] with charge iteration[25] were performed using an in-house modified program in conjunction with the Spartan v.3.1.2 builder.[26] The molecular structures of the species investigated were minimized using the Spartan MM2 molecular mechanics routine with Ru−N distances constrained according to the crystal structure of β-[Ru(bpy)(**5**)$_2$](PF$_6$)$_2$.

X-ray Structure Determination. Single-crystals of β-[Ru(bpy)-(**5**)$_2$](PF$_6$)$_2$ were grown from MeOH at room temperature. X-ray diffraction was carried out on a Siemens R3m/V diffractometer with Mo Kα radiation (λ = 0.710 73 Å) at room temperature, using the $\omega/2\theta$ scan mode. The data were corrected for Lorentz and polarization effects. No absorption correction was performed. Because of the inherent systematic absences, only 2920 observed reflections were collected. Except for H, at calculated positions according to a riding model, and except for the disordered F (see below), a fully anisotropic refinement of all atoms was performed by a full-matrix, weighted least-squares method on F^2 using SHELXL-93.[38] Details of the data collection and refinement, atomic coordinates, thermal parameters, and bond lengths and angles are available in the Supporting Information. The −COOEt groups showed substantial uncertainty (Figure 2), but treating them as disordered was not necessary for our purposes. Both PF$_6^-$ groups were found to be substantially disordered. One group was modeled as a P atom on a fully occupied site and two sets of F atoms with fitted occupancies of 52% and 48%. The other was treated as a P atom on its octahedral center, two axial F on fully occupied sites, and two sets of equatorial F atoms, with fitted occupancies of 59% and 41%. All four PF$_6^-$ sets were imposed octahedral geometries with P−F distances of 1.53 Å and were treated as rigid groups. The final weighted $R(F^2)$ value was 0.2573, corresponding to an $R(F)$ value of 0.1031 for data where $F > 4\sigma(F)$.

[Ru(bpy)$_2$L](PF$_6$)$_2$ Complexes. (a) [Ru(bpy)$_2$1](PF$_6$)$_2$. *cis*-Ru(bpy)$_2$-Cl$_2$·2H$_2$O (1.04 g, 2.0 mmol) and 2*H*-3-(pyridin-2-yl)-4,5,6,7-tetrahydroindazole **1** (0.42 g, 2.1 mmol) were heated under reflux in MeOH or MeOH−H$_2$O (4:1) overnight. The solvent was removed under reduced pressure, the residue taken up in H$_2$O, and the solution filtered free of any unreacted ligand. The filtrate was treated with NH$_4$PF$_6$ (0.68 g, 4.2 mmol) to give a yellow-orange precipitate. Recrystallization from MeOH gave 1.2 g (66%) of orange crystals. Anal. Calcd for C$_{32}$H$_{29}$F$_{12}$N$_7$P$_2$Ru·H$_2$O: C, 41.75; H, 3.39; N, 10.65. Found: C, 41.31; H, 3.38; N, 10.48. ^{1}H-NMR: δ 1.78−1.89 (m, 4H), 2.57 (m, 1H), 2.67 (m, 1H), 2.91 (m, 2H), 11.27 (b s, 1H) ppm. ^{13}C-NMR: δ 21.70, 21.83, 22.32, 23.13 ppm.

(b) [Ru(bpy)$_2$2](PF$_6$)$_2$. By use of the same procedure as for **1**, the crude product from *cis*-Ru(bpy)$_2$Cl$_2$·2H$_2$O (0.24 g, 0.46 mmol) and 1-methyl-3-(pyridin-2-yl)-4,5,6,7-tetrahydroindazole **2** (0.11 g, 0.50 mmol) was purified by column chromatography, using 5% MeOH in CHCl$_3$ as eluent, yielding 0.28 g (66%). Anal. Calcd for C$_{33}$H$_{31}$F$_{12}$N$_7$P$_2$-Ru: C, 43.24; H, 3.41; N, 10.70. Found: C, 43.20; H, 3.33; N, 10.79. ^{1}H-NMR: δ 1.76−1.89 (m, 4H), 2.54 (m, 1H), 2.66 (m, 1H), 2.87 (s, 3H), 2.91 (m, 2H) ppm. ^{13}C-NMR δ 22.08, 22.36, 22.62, 22.92, 35.54 ppm.

(c) [Ru(bpy)$_2$3](PF$_6$)$_2$. Using the same procedure as for **1**, *cis*-Ru-(bpy)$_2$Cl$_2$·2H$_2$O (0.26 g, 0.50 mmol) and 1-phenyl-3-(pyridin-2-yl)-4,5,6,7-tetrahydroindazole (**3**) (0.14 g, 0.51 mmol) provided 0.35 g (72%). Anal. Calcd for C$_{38}$H$_{33}$F$_{12}$N$_7$P$_2$Ru·H$_2$O: C, 45.79; H, 3.54; N, 9.84. Found: C, 46.17; H, 3.36; N, 9.82. ^{1}H-NMR: δ 1.77−1.90 (m, 4H), 2.20 (m, 1H), 2.38 (m, 1H), 3.03 (m, 2H), 6.09 (d, 1H, Ph), 6.85 (b, 1H, Ph), 7.11 (b, 2H, Ph), 7.30 (b, 1H, Ph) ppm. ^{13}C-NMR: δ 22.11, 22.28, 22.86, 22.90, 128.84 (C-4″), 130.6 (C-3″, C-5″), 131.96 (C-2″), 136.88 (C-1″), 137.57 (C-6″) ppm.

(d) [Ru(bpy)$_2$4](PF$_6$)$_2$. As for **1**, *cis*-Ru(bpy)$_2$Cl$_2$·2H$_2$O (0.26 g, 0.50 mmol) and 1-(4-(methoxycarbonyl)phenyl)-3-(pyridin-2-yl)-4,5,6,7-tetrahydroindazole (**4**) (0.17 g, 0.51 mmol) produced 0.35 g (68%) after recrystallization from MeOH. Anal. Calcd for C$_{40}$H$_{35}$F$_{12}$N$_7$O$_2$P$_2$Ru·H$_2$O: C, 45.55; H, 3.54; N, 9.30. Found: C, 45.57; H, 3.37; N, 9.17. ^{1}H-NMR δ 1.82−1.89 (m, 4H), 2.30 (m, 1H), 2.45 (m, 1H), 3.07 (m, 2H), 3.92 (s, 3H), 6.27 (b d, 1H, Ph), 7.42 (b, 2H, Ph), 7.68 (b, 1H, Ph) ppm. ^{13}C-NMR: δ 22.29, 22.40, 23.00 (2C), 53.33, 131.68 (C-3″, C-5″), 133.64 (C-2″), 137.54 (C-6″), 140.66 (C-1″), 166.29 (C═O) ppm.

(e) [Ru(bpy)$_2$5](PF$_6$)$_2$. As for **1**, *cis*-Ru(bpy)$_2$Cl$_2$·2H$_2$O (0.26 g, 0.50 mmol) and 1-(4-(ethoxycarbonyl)phenyl)-3-(pyridin-2-yl)-4,5,6,7-tetrahydroindazole **5** (0.17 g, 0.49 mmol) produced 0.30 g (58%) with recrystallization from MeOH. Anal. Calcd for C$_{41}$H$_{37}$F$_{12}$N$_7$O$_2$P$_2$Ru·2H$_2$O: C, 45.31; H, 3.80; N, 9.02. Found: C, 45.52; H, 3.49; N, 9.01. ^{1}H-NMR: δ 1.38 (t, 3H), 1.79−1.86 (m, 4H), 2.27 (m, 1H), 2.42 (m, 1H), 3.04 (m, 2H), 4.34 (q, 2H), 6.23 (b d, 1H, Ph), 7.4 (b, 2H, Ph), 7.69 (b d, 1H, Ph) ppm. ^{13}C-NMR: δ 14.60, 22.11, 22.25, 22.83, 22.85, 62.49, 128.11 (C-4″), 131.42, 131.53, 133.65 (C-2″), 137.30 (C-6″), 140.43 (C-1″), 165.61 (C═O) ppm.

(f) [Ru(bpy)$_2$6](PF$_6$)$_2$. As for **1**, *cis*-Ru(bpy)$_2$Cl$_2$·2H$_2$O (0.26 g, 0.50 mmol) and 1-(4-carboxyphenyl)-3-(pyridin-2-yl)-4,5,6,7-tetrahydroindazole (**6**) (0.19 g, 0.59 mmol) provided 0.40 g (78%). Anal. Calcd for C$_{39}$H$_{33}$F$_{12}$N$_7$O$_2$P$_2$Ru·H$_2$O: C, 45.01; H, 3.39; N, 9.42. Found: C, 44.96; H, 3.43; N, 9.31. ^{1}H-NMR: δ 1.78−1.87 (m, 4H), 2.24 (m, 1H), 2.43 (m, 1H), 3.03 (m, 2H), 6.24 (b, 1H Ph), 7.43 (b, 2H, Ph), 7.70 (b, 1H, Ph) ppm. ^{13}C-NMR: δ 22.32, 22.43, 23.04, 132.00, 137.58, 140.51 ppm.

[Ru(bpy)L$_2$](PF$_6$)$_2$ Complexes. (a) α-[Ru(bpy)(4)$_2$](PF$_6$)$_2$. Ru-(DMSO)$_4$Cl$_2$ (0.12 g, 0.25 mmol) was treated with 0.17 g (0.51 mmol)

(36) Krejcik, M.; Danek, M.; Hartl, F. *J. Electroanal. Chem. Interfacial Electrochem.* **1991**, *317*, 179.
(37) Tse, Y. H. Ph.D. Thesis, York University, Toronto, Canada, 1994.
(38) Sheldrick, G. M. *J. Appl. Crystallogr.* in preparation. Sheldrick, G. M. In *Crystallographic Computing 6*; Flack, H. D., Párkányi, L. & Simon, K., Eds.; Oxford University Press: Oxford, U.K.; 1993; pp 111−122.

of 1-(4-(methoxycarbonyl)phenyl)-3-(pyridin-2-yl)-4,5,6,7-tetrahydroindazole (**4**) in refluxing MeOH overnight. Then, 0.039 g (0.25 mmol) of 2,2′-bipyridine was added, and the solution was again heated at reflux overnight. MeOH was removed under reduced pressure, and water was added to dissolve the residue. After filtration, 0.10 g (0.60 mmol) of NH_4PF_6 was added to precipitate 0.29 g of crude orange solid. An aliquot (70.6 mg) of this solid was chromatographed on a column, using first 5% MeOH in EtOAc and then 5% MeOH in $CHCl_3$ as eluents. The first fraction amounted to 12.0 mg of *mer*-[Ru(**4**)$_3$](PF$_6$)$_2$. The second provided 35.5 mg (48% yield) of the desired α-[Ru(bpy)(**4**)$_2$](PF$_6$)$_2$, and the third gave 20.3 mg of [Ru(bpy)$_2$**4**](PF$_6$)$_2$. Anal. Calcd for $C_{50}H_{46}F_{12}N_8O_4P_2Ru\cdot 2H_2O$: C, 48.04; H, 4.03; N, 8.96. Found: C, 48.31; H, 3.95; N, 8.68. ^{1}H-NMR: δ 1.79−1.88 (m, 4H), 2.26 (m, 1H), 2.42 (m, 1H), 2.90 (m, 2H), 3.90 (s, 3H), 6.78 (d, 1H), 7.19 (d, 1H), 7.47 (d, 1H), 7.65 (d, 1H) ppm. ^{13}C-NMR: δ 22.20, 22.45, 23.02, 53.34, 128.26, 129.42, 130.66, 131.13, 133.37, 140.22, 166.23 ppm.

(b) α-[Ru(bpy)(5)$_2$](PF$_6$)$_2$ from Ru(DMSO)$_4$Cl$_2$. Using the same procedure as for **4**, 1-(4-(ethoxycarbonyl)phenyl)-3-(pyridin-2-yl)-4,5,6,7-tetrahydroindazole **5** (0.17 g, 0.49 mol) provided 0.28 g of crude products. Analogous chromatography of 75 mg of material provided 14 mg of *mer*-[Ru(**5**)$_3$](PF$_6$)$_2$, 40 mg (48% yield) of α-[Ru(bpy)(**5**)$_2$](PF$_6$)$_2$, and 17 mg of [Ru(bpy)$_2$**5**](PF$_6$)$_2$. Anal. Calcd for $C_{52}H_{50}F_{12}N_8O_4P_2Ru\cdot H_2O$: C, 49.57; H, 4.16; N, 8.89. Found: C, 49.18; H, 4.14; N, 8.73. ^{1}H-NMR: δ 1.40 (t, 3H), 1.84−2.00 (m, 4H), 2.42 (m, 1H), 2.52 (m, 1H), 2.89 (m, 2H), 4.36 (q, 2H), 6.76 (d, 1H), 7.19 (d, 1H), 7.46 (d, 1H), 7.65 (d, 1H) ppm. ^{13}C-NMR: δ 14.64, 22.15, 22.41, 22.97, 62.53, 128.21, 129.34, 130.56, 130.99, 133.58, 140.10, 165.70 (C═O) ppm.

(c) β-[Ru(bpy)(5)$_2$](PF$_6$)$_2$ from Ru(bpy)Cl$_3$·H$_2$O. A mixture of Ru(bpy)Cl$_3$·H$_2$O (0.38 g, 1.0 mmol) and 1-(4-(ethoxycarbonyl)phenyl)-3-(pyridin-2-yl)-4,5,6,7-tetrahydroindazole **5** (0.69 g, 2.0 mmol) was heated at reflux in MeOH−H$_2$O (4:1) overnight. This was freed of solvents under reduced pressure, the residue taken up in H_2O, and the solution filtered to remove any unreacted ligand. NH_4PF_6 (0.50 g, 3.0 mmol) was added to precipitate 1.23 g of orange solid. After dissolution in 1:9 MeOH-$CHCl_3$ and cooling in a refrigator, 0.46 g (37%) of pure β-[Ru(bpy)(**5**)$_2$](PF$_6$)$_2$ was obtained. Anal. Calcd for $C_{52}H_{50}F_{12}N_8O_4P_2Ru$: C, 50.29; H, 4.06; N, 9.02. Found: C, 50.04; H, 4.06; N, 9.00. ^{1}H-NMR: δ 1.38 (t, 3H), 1.7−1.85 (m, 4H), 2.16−2.29 (m, 2H), 2.95 (t, 2H), 4.34 (q, 2H), 6.04 (d, 1H), 7.21 (b d, 1H), 7.44 (b, 1H), 7.51 (b d, 1H) ppm. ^{13}C-NMR: δ 14.60, 21.97, 22.11, 22.72, 62.47, 127.91, 131.13, 131.35, 133.56, 139.76, 165.52 ppm. A mixture (1:1) of α- and γ-[Ru(bpy)(**5**)$_2$](PF$_6$)$_2$, some [Ru(bpy)$_2$**5**](PF$_6$)$_2$, and some [Ru(**5**)$_3$](PF$_6$)$_2$ were also isolated from the crude product by TLC and identified by ^{1}H-NMR.

(d) α-[Ru(bpy)(6)$_2$](PF$_6$)$_2$. As for **4**, **7** (0.16 g, 0.5 mmol) yielded 0.25 g of crude products in 78% yield (see text) containing α-[Ru(bpy)(**6**)$_2$](PF$_6$)$_2$ (estimated yield 66%). ^{1}H-NMR: δ 6.75 (d, 1H), 7.18 (d, 1H), 7.49 (d, 1H), 7.66 (d, 1H) ppm.

(e) β-[Ru(bpy)(6)$_2$](PF$_6$)$_2$. A solution of β-[Ru(bpy)(**5**)$_2$](PF$_6$)$_2$ (0.25 g, 0.20 mmol) in 8 mL of 0.1 M NaOH and 25 mL of water was heated under reflux overnight. After the water was evaporated under reduced pressure, the residue was extracted with acetonitrile and the solution filtered free of any insoluble material. The filtrate was evaporated to remove CH_3CN, and the residue was then taken up in H_2O. Acidification with 0.1 M HCl provided 0.21 g (89%) of pure β-[Ru(bpy)(**6**)$_2$](PF$_6$)$_2$. Anal. Calcd for $C_{48}H_{42}F_{12}N_8O_4P_2Ru\cdot H_2O$: C, 47.89; H, 3.68; N, 9.31. Found: C, 47.74; H, 3.62; N, 9.24. ^{1}H-NMR: δ 1.74−1.85 (m, 4H), 2.17−2.27 (m, 2H), 2.95 (t, 2H), 6.04 (d, 1H), 7.19 (b d, 1H), 7.45 (b, 1H), 7.51 (b d, 1H) ppm. ^{13}C-NMR δ 21.99, 22.12, 22.73, 22.78, 125.29, 127.80, 131.45, 131.65, 133.45, 139.82, 166.15 ppm.

[RuL$_3$](PF$_6$)$_2$ Complexes. (a) *mer*- and *fac*-[Ru(1)$_3$](PF$_6$)$_2$. A mixture of Ru(DMSO)$_4$Cl$_2$ (0.14 g, 0.29 mmol) and **1** (0.18 g, 0.90 mmol) was heated at reflux in MeOH−H$_2$O (4:1) overnight. The MeOH was evaporated at reduced pressure, and the residue was filtered to remove any unreacted ligand. The filtrate was then treated with NH_4PF_6 (0.11 g, 0.67 mmol) to give 0.27 g of a yellow solid. After dissolution in MeOH (10 mL), trituration with ether and cooling in a refrigerator resulted in the precipitation of pure *mer*-[Ru(**1**)$_3$](PF$_6$)$_2$ (0.17 g, 59%). Anal. Calcd for $C_{36}H_{39}F_{12}N_9P_2Ru\cdot CH_3OH\cdot H_2O$: C, 42.78; H, 4.37; N, 12.13. Found: C, 42.73; H, 4.52; N, 11.86. ^{1}H-NMR: δ 1.73−1.93 (m, 12H), 2.63−2.72 (m, 6H), 2.90 (m, 6H), 11.20 (s, 1H), 11.24 (s, 2H) ppm. ^{13}C-NMR: δ 21.63, 21.80, 22.31, 23.08 ppm. The mother liquor was evaporated to provide pure *fac*-[Ru(**1**)$_3$](PF$_6$)$_2$ (0.10 g, 35%). An analytical sample was obtained by recrystallization from MeOH. Anal. Calcd for $C_{36}H_{39}F_{12}N_9P_2Ru\cdot 3CH_3OH$: C, 43.18; H, 4.74; N, 11.62. Found: C, 43.05; H, 4.35; N, 11.26. ^{1}H-NMR: δ 1.76−1.89 (m, 4H), 2.58 (m, 1H), 2.68 (m, 1H), 2.88 (m, 2H), 12.34 (b s, 1H) ppm. ^{13}C-NMR: δ 21.68, 22.02, 22.46, 23.24 ppm.

(b) *mer*-[Ru(2)$_3$](PF$_6$)$_2$. As for **1**, Ru(DMSO)$_4$Cl$_2$ (0.17 g, 0.35 mmol) and **2** (0.25 g, 1.2 mmol) provided 0.25 g (69%) of pure *mer* product. Anal. Calcd for $C_{39}H_{45}F_{12}N_9P_2Ru$: C, 45.44; H, 4.40; N, 12.23. Found: C, 45.82; H, 4.30; N, 12.55. ^{1}H-NMR: δ 1.76−1.92 (m, 12H), 2.57 (m, 3H), 2.71 (m, 3H), 2.82−2.94 (m, 6H), 2.83 (s, 3H), 2.92 (s, 3H), 2.94 (s, 3H) ppm. ^{13}C-NMR: δ 21.96, 22.02, 22.34, 22.41, 22.57, 22.67, 22.88, 22.93, 35.10, 35.27, 35.51 ppm.

(c) *mer*-[Ru(3)$_3$](PF$_6$)$_2$. As for **1**, Ru(DMSO)$_4$Cl$_2$ (0.16 g, 0.33 mmol) and **3** (0.31 g, 1.1 mmol) produced 0.23 g (57%) of the *mer* complex. Anal. Calcd for $C_{54}H_{51}F_{12}N_9P_2Ru$: C, 53.29; H, 4.22; N, 10.36. Found: C, 52.83; H, 4.29; N, 10.31. ^{1}H-NMR: δ 1.63−2.96 (CH$_2$), 5.97 (d, 1H, Ph), 6.23 (d, 1H, Ph), 6.38 (d, 1H, H-2″), 6.97 (d, 1H, H-3″), 7.07 (t, 1H, H-4″), 6.85 (d, 1H, H-5″), 7.02 (d, 1H, H-6″), 7.19 (b, 1H, Ph), 7.42 (b, 1H, Ph) ppm. ^{13}C-NMR: δ 21.89, 21.97, 22.22, 22.37, 22.63, 22.79, 22.85, 22.97, 23.00, 128.00, 128.57, 129.06, 129.42, 129.63, 129.89, 130.04, 130,17, 131.52, 131.55, 131.84, 136.08, 136.23, 136.69 ppm.

(d) *mer*-[Ru(4)$_3$](PF$_6$)$_2$. As for **1**, Ru(DMSO)$_4$Cl$_2$ (0.049 g, 0.10 mmol) and **4** (0.11 g, 0.33 mmol) gave 0.070 g (50%) of *mer* product. Anal. Calcd for $C_{60}H_{57}F_{12}N_9O_6P_2Ru$: C, 51.80; H, 4.13; N, 9.06. Found: C, 52.28; H, 4.19; N, 8.88. ^{1}H-NMR: δ 1.67−2.95 (CH$_2$), 3.86, 3.91, 3.94, 6.04 (b d, 1H, Ph), 6.44 (b, 1H, Ph), 6.57 (dd, 1H, H-2″), 6.93 (b, 1H), 7.05 (dd, 1H, H-3″), 7.36 (d, 1H, H-5″), 7.41 (b, 1H), 7.61 (d, 1H, H-6″), 7.73 (b, 1H), 8.03 (b, 1H) ppm. ^{13}C-NMR: δ 21.80, 21.96, 22.16, 22.26, 22.53, 22.57, 22.71, 22.83, 22.99, 128.15, 128.92, 129.66, 130.20, 130.43, 130.77, 130.86, 130.96, 132.98, 133.11, 133.31, 137.42, 166.13, 166.18, 166.39 (C═O) ppm.

(e) *mer*-[Ru(5)$_3$](PF$_6$)$_2$. As for **1**, Ru(DMSO)$_4$Cl$_2$ (0.16 g, 0.33 mmol) and **5** (0.38 g, 1.1 mmol) provided 0.36 g (76%) of this *mer* complex. Anal. Calcd for $C_{63}H_{63}F_{12}N_9O_6P_2Ru$: C, 52.80; H, 4.43; N, 8.80. Found: C, 52.50; H, 4.35; N, 8.87. ^{1}H-NMR: δ 1.33 (t, 3H), 1.41 (t, 3H), 1.43 (t, 3H), 1.68−2.98 (CH$_2$), 4.32 (q, 2H), 4.37 (q, 2H), 4.39 (q, 2H), 6.05 (d, 1H), 6.43 (b, 1H), 6.56 (dd, 1H, H-2″), 6.96 (b, 1H), 7.04 (dd, 1H, H-3″), 7.36 (d, 1H, H-5″), 7.40 (b, 1H), 7.60 (d, 1H, H-6″), 7.65 (b, 1H), 7.73 (b, 1H), 7.77 (b, 1H), 8.04 (b, 1H) ppm. ^{13}C-NMR: δ 14.48, 14.63, 14.63, 21.76, 21.95, 22.03, 22.15, 22.27, 22.51, 22.60, 22.71, 22.81, 22.97, 62.53, 62.59, 62.72, 128.19, 128.86, 128.95, 129.61, 130.31, 130.68, 130.79, 130.93, 133.31, 133.39, 133.60, 137.36, 165.62, 165.66, 165.91 (C═O) ppm.

(f) *mer*-[Ru(6)$_3$](PF$_6$)$_2$. As for **1**, Ru(DMSO)$_4$Cl$_2$ (0.19 g, 0.39 mmol) and **6** (0.38 g, 1.2 mmol) produced 0.29 g (55%) of *mer* product. Anal. Calcd for $C_{57}H_{51}F_{12}N_9O_6P_2Ru$: C, 50.75; H, 3.81; N, 9.34. Found: C, 50.51; H, 4.11; N, 9.26. ^{1}H-NMR (DMSO-d_6): δ 1.73−1.91 (m), 2.22−2.32 (m), 2.89−3.05 (m), 6.02 (d, 1H), 6.69 (b, 1H), 6.80 (d, 1H), 7.02 (b, 1H), 7.13 (d, 1H), 7.25 (d, 1H), 7.48 (b, 1H), 7.54 (d, 1H), 7.93 (b, 1H), 7.96 (b, 1H) ppm. ^{13}C-NMR (DMSO-d_6): δ 20.46, 20.55, 20.63, 20.80, 20.97, 21.16, 21.28, 21.39, 21.56, 21.65, 116.35, 116.57, 116.78, 127.00, 127.40, 127.85, 128.18, 128.51, 129.00, 129.50, 136.24, 166.06, 166.10, 166.32 ppm.

Acknowledgment. The authors are grateful to D. V. Stynes for invaluable assistance in acquiring the X-ray crystal structure, to Dr A. A. Vlček for useful discussions, and to the Natural Sciences and Engineering Research Council for funding.

Supporting Information Available: Tables of crystallographic data collection and structure solution information, atomic coordinates and equivalent isotropic displacement coefficients, bond lengths, bond angles, and anisotropic displacement coefficients, a table of ^{13}C-NMR shifts for aromatic signals with positional assignments, CV plots for [Ru(**3**)$_3$](PF$_6$)$_2$ (room temperature and −85 °C) and [Ru(bpy)(**5**)$_2$](PF$_6$)$_2$, and UV−visible spectra of [Ru(bpy)$_2$**5**](PF$_6$)$_2$ undergoing reduction to [Ru(bpy)$_2$**5**]$^+$ (16 pages). Ordering information is given on any current masthead page.

IC950694Q